Radiative emission from air thermal plasmas with vapour of Cu or W

V Aubrecht, M Bartlova, O Coufal

Radiative emission from air thermal plasmas with vapour of Cu or W

V Aubrecht, M Bartlova and O Coufal

Brno University of Technology,
Faculty of Electrical Engineering and Communication,
Technicka 8, 616 00 Brno, Czech Republic

E-mail: aubrecht@feec.vutbr.cz

PACS numbers: 52.25.Os

Submitted to: *J. Phys. D: Appl. Phys.*

Abstract. The paper deals with net emission coefficients of radiation of air thermal plasmas with admixtures of copper and tungsten as a function of the plasma temperature up to 25 000 K and the arc radius (0.01 to 10 cm) at various pressures. The net emission coefficients are calculated for various equilibrium compositions (mole fractions of Cu and W) of the plasma. Calculations take into account continuum and line radiations, special attention has also been taken to the fraction of radiation that is below threshold of 120 nm. From the results follows that presence of metallic vapour increases net emission coefficients even at low temperatures below 10 000 K.

1. Introduction

It has been reported by several authors that the presence of small amounts of metallic vapours substantially modifies properties of thermal plasmas, including radiation heat transfer [1]–[6]. Even small amount of the contamination by metallic vapours may have a strong effect on the radiative heat transfer due to the relatively low ionization potential of such admixtures. Calculation of the radiation absorption and/or emission is very strongly dependent on the species involved and particular spectral data like energy levels, oscillator strengths, cross sections, line broadening and continuum emission mechanisms. In this paper we present the calculation of the net emission coefficient for mixtures of air thermal plasma and vapour of copper and tungsten. The choice of mixtures was guided by usual applications (transferred arc with copper anode, tungsten inert gas welding, plasma spraying of metallic particles). The presence of electrode material in an arc plasma and its vaporization is of great importance in studies of electrode phenomena with the final goal of better performance of circuit breakers.

The radiation heat transfer have to be calculated as a function of wavelength spanning from the infra-red to the far ultraviolet region of the spectrum. Exact

calculations of radiations properties are very complex and time consuming so it is desirable to account for radiation losses in an approximate way. Between existing approximation methods, the method of partial characteristics [7] and use of the net emission coefficients are mostly used in computational plasma flow dynamics. Both methods are based on an assumption of local thermodynamic equilibrium. In the present paper we report calculation of the net emission coefficient ε_N as defined by Lowke [8].

The net emission coefficients are defined for an isothermal and homogeneous plasma. They can be used for prediction of the amount of radiation energy losses as radiative source term representing divergence of radiation flux $\mathrm{F_R}$:

$$\nabla \mathrm{F_R} = 4\pi\varepsilon_N \tag{1}$$

The net emission coefficient corresponds to the difference between the power radiated by a volume unit and the radiation proceeding from other regions of the plasma and absorbed in this volume unit. These coefficients largely determine axial plasma temperatures above 8 000 K. To account for a balance between emission and absorption at lower temperatures with steep gradients, the method of net emission coefficients is not valid. Furthermore, molecules at lower temperatures are not fully dissociated and play an important role which increases with the plasma pressure [9, 10]. Even though the use of the net emission coefficients cannot precisely account for an absorption in the outer part of the arc with steep temperature gradient, it is widely used in complex computations of a plasma flow.

Successful application of the net emission coefficients in computational flow dynamics has been reported by several authors. For example, Lindmayer [11] applied the method of the net emission coefficients to the prediction of radiation transfer in modelling of switching arc in low voltage circuit breakers. Zhang [12] used the net emission coefficients for approximate radiation transport model in theoretical investigation of the arc in a supersonic nozzle. The computed results has been shown in good agreement with experiments.

In this paper, the net emission coefficients of Air+Cu and Air+W plasmas at temperatures from 3000 to 25 000 K are presented for dimensions from 0 to 10 cm at various pressures up to 20 bars. To validate our own calculation, calculated results of the net emission coefficients for the plasmas of Air+Cu are compared with those published in [1]. Even that we have used different approach for the spectral lines treatment, comparison shows reasonable agreement.

2. Plasma Composition

Composition of the air plasma was computed using `Tmdhet` computer code with input data `species` which is part of the database system `TheCoufal`, available at http://www.feec.vutbr.cz/∼coufal/ [13]. The calculation of composition is based on the method of minimizing the Gibbs energy of a system. The air was assumed at US standard atmosphere sea level [14]. Volume concentration of gases in pure air was as follows:

Table 1. Volume concentration of gases in pure air.

N_2	78.0840	vol%
O_2	20.9476	vol%
Ar	0.9370	vol%
CO_2	0.0314	vol%

The volume amount of substance (in mol) of the pure air elements was the same in both systems:

Table 2. Amount of substance of elements in pure air.

element	amount
C	0.0031
N	15.6168
O	4.1958
Ar	0.0937

We have treated two plasma systems denoted as Air+Cu and Air+W which differ by concentration of copper and tungsten admixtures. For each system we have calculated 3 variants of the plasma composition so that amount of substance of copper and tungsten was 1, 5 and 10 vol%, respectively, i.e. in each variant there is equal number of copper and tungsten particles.

The used amounts of substance (in mol) of Cu and W for variants 1 to 3 are presented in table 3.

The following assumption has been made for the calculation of the plasma compositions:

- The system is in the state of thermodynamic equilibrium and its temperature T satisfies the relation $T_\mathrm{a} \leq T \leq 50$ kK, where $T_\mathrm{a} = 298.15\,\mathrm{K}$ is the standard ambient temperature;
- The gaseous phase satisfies the state equation $pV_m = RT$,where p is the pressure in the system, and V_m is the molar volume;
- The gaseous phase is a thermal plasma (electrically neutral gas as a whole in a state of thermodynamic equilibrium) if there are electrically charged particles in

Table 3. Amount of substance of copper and tungsten in 3 treated variants of the plasma composition.

variant	amount of Cu	amount of W
1	0.046042	0.046042
2	0.239902	0.239902
3	0.506459	0.506459

the system;

- The behaviour of phases in a heterogeneous system is ideal.

As an example, the equilibrium compositions of air with admixture of 10 volume percent (vol%) of copper and tungsten at a pressure of 1 atm are respectively presented in figure 1. Only species with significant contribution to the calculated radiation properties are plotted in the figure.

Composition variants of both systems Air+Cu and Air+W differ mainly in the amount of Cu and W atomic, ionic and molecular species. Comparison of the variants for Air+Cu and Air+W with respect to these species is presented in figure 2.

3. Absorption of radiation

The mechanisms of absorption of radiation by matter are bound-bound (line) absorption (bb), bound-free photo-absorption(bf) and free-free absorption(ff). In line absorption, an electron in a bound state is excited to another bound state of higher energy by the absorption of a photon. In photo-absorption, the electron is ejected from the atom (or ion) and goes into one of the continuum free energy states. In free-free absorption, an electron in a free state makes a transition to another free state of higher energy with the absorption of a photon. Similar processes occur when the material is composed of molecules. Molecular processes are somewhat more complicated because of the extra degrees of freedom (vibrational and rotational) that are present when atoms join together to form molecules. Total absorption coefficient κ is given as a linear sum of all three processes

$$\kappa(\nu, T, p) = \kappa^{ff} + \kappa^{bf} + \kappa^{bb} \tag{2}$$

An exact calculation of absorption coefficients represents a complex task since the population level of each quantum state of the matter together with transition probabilities of all processes mentioned above must be determined. To calculate the transition probabilities (absorption cross sections), the radial wave functions of all free and bound electronic states must be known and corresponding Schrödinger equations have to be solved. Nevertheless, some experimental data can be used and in case of lack of these simplifications semi-empirical methods exist.

Absorption coefficients were calculated using the methods of Liebermann and Lowke [15, 16].

3.1. Continuous radiation

The absorption of continuous radiation consists of bound-free photo-absorption and free-free absorption. In bound-free (ionization) process, a photon is absorbed by an atom, the electron is ejected and a positive ion arises. For a given species, the corresponding cross-section is assumed non-dependent on both the plasma temperature and pressure.

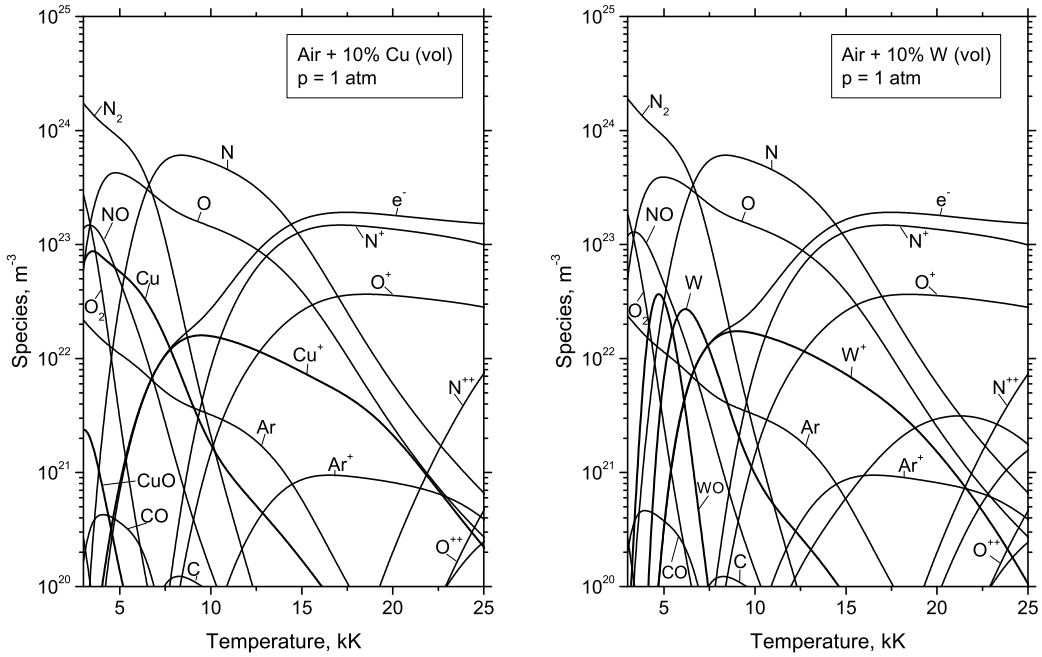

(a) Air+Cu (b) Air+W

Figure 1. Concentration of species in the air plasma with 10 vol% of Cu (a) and W (b) at a pressure of 1 atm.

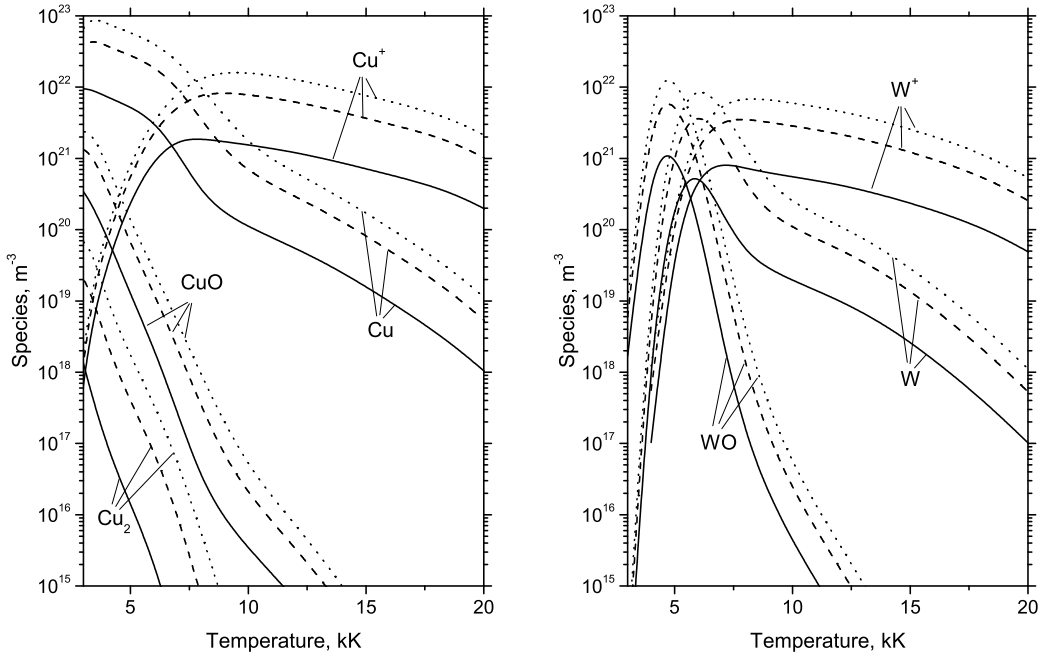

(a) Air+Cu (b) Air+W

Figure 2. Concentration of Cu (a) and W (b) species at different variants of composition systems Air+Cu and Air+W at a pressure of 1 atm.
——variant 1: 1 vol%, - - - -variant 2: 5 vol%, ·····variant 3: 10 vol%

The spectral absorption coefficient of the process is related to the photo-ionization cross section $\sigma^a_{\nu,i}$ by

$$\kappa^{bf}_{\nu,i} = \sigma^a_{\nu,i} N^a_i, \tag{3}$$

where N^a_i is the population density of the i-th electronic state E^a_i of the absorbing species a. Thus, at a given spectral frequency, plasma temperature and pressure, the bound-free spectral absorption coefficient is

$$\kappa^{bf}_{\nu} = \sum_a \sum_i \sigma^a_{\nu,i} N^a_i \tag{4}$$

where the summation is over all atoms and ions having energy states such that $h\nu \geq E^a_\infty - E^a_i$, where E^a_∞ is the ionization energy.

Photo-ionization cross sections for the ground states of neutral atoms and ions were calculated using analytic fits of theoretical cross sections from the "Opacity Project" [17]. The cross sections for the lowest excited levels of neutral atoms were calculated using the quantum defect method of Burges and Seaton [18]. The higher exited levels of neutral atoms and all excited states of ions were treated using Coulomb approximation for hydrogen-like species [19]. The energy levels tabulated in [20] were used for all atoms and ions under consideration. The hydrogen-like approximation was used for treatment of free-free transitions.

In contrast to bound electrons of a given level, free electrons contribute to the absorption coefficient at all frequencies. The relative importance of bound-free and free-free absorption depends on the state of ionization. At low temperatures, there are very few free electrons, and bound-free absorption dominates. At very high temperatures, most electrons are free and for radiation frequencies under consideration (infrared, visible, ultraviolet) free-free absorption is dominant. However, for heavy elements free-free absorption is usually much smaller than photo-absorption for the usual range of temperatures and frequencies encountered in radiative transfer work.

Comparisons of calculated continuum absorption coefficients as a function of radiation frequency for various plasma systems (air, air with 10 vol% of copper and tungsten, respectively) are shown in figure figure 3a) for the plasma temperature of 7000 K and in figure 3b) for 20 000 K at atmospheric pressure. In all presented cases, dominant role is played by bound-free (photo-recombination) effect. Molecular continuum is taken account through averaged rotational spectra of individual band systems according to the method described in section 3.3. Molecular species contribute to the total absorption coefficients slightly at lower tempertaures below 10 kK at radiation frequencies up to 2.5×10^{15} s^{-1} [10]. It can be seen from the figure that the absorption coefficient raises with admixture of either Cu or W in comparison to the one in the pure air plasma. At the temperature of 20 000 K, admixture of tungsten does not contribute to the increasing of the absorption above the threshold of 2.5×10^{15} s^{-1} which is due to small values of photo-ionization cross sections of W^+ ions with respect to N and O ions.

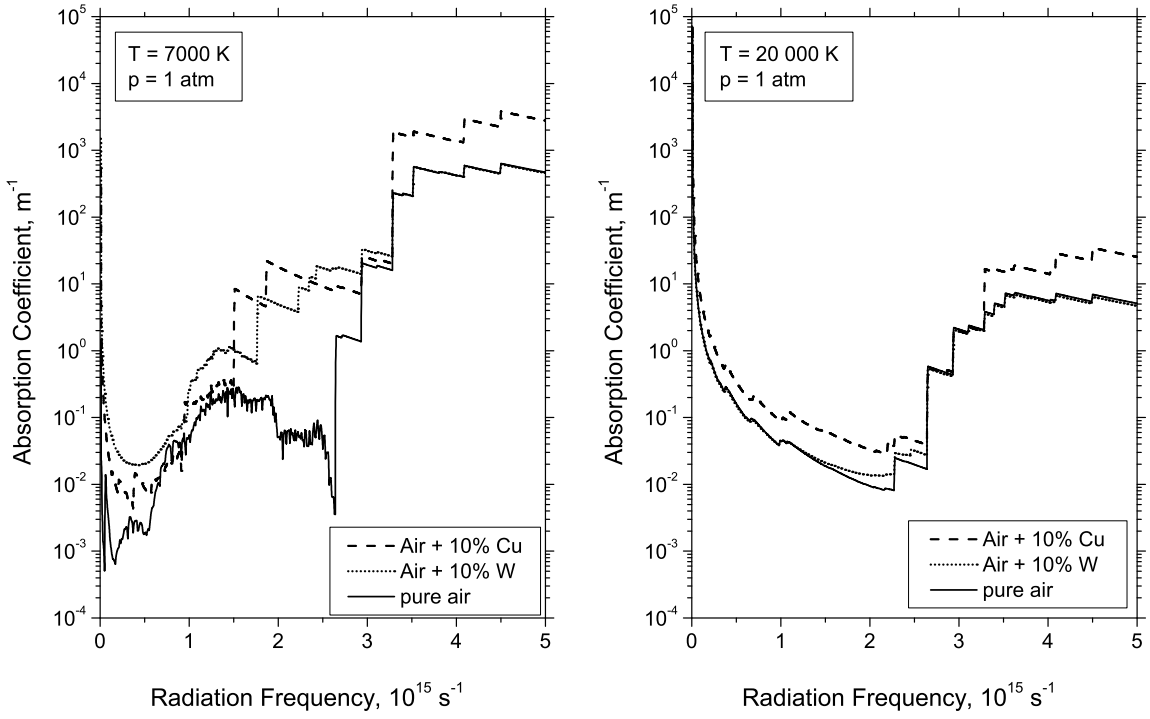

(a) T = 7000 K (b) T = 20 000 K

Figure 3. Continuum absorption coefficient for the air thermal plasma with admixtures of Cu and W at temperatures of 7000 K and 20 000 K, respectively.

3.2. Discrete radiation

In line absorption, an electron in bound state is excited to another bound state of higher energy by the absorption of a quantum of radiation (photon). The frequency of the absorption line is given by Bohr's relation

$$h\nu_{mn} = \frac{hc}{\lambda_{mn}} = E_m - E_n, \tag{5}$$

where E_n and E_m are the lower and higher energy states, respectively. The transition probability of this process can be found by solution of the Schrödinger equation with non-relativistic Hamiltonian of the system comprising an atom and a radiation field. The probabilities are usually expressed through electric dipole line strengths S_{mn} or absorption oscillator strengths f_{mn}, these quantities are most often found in the atomic tables. Due to perturbations, the energy levels are smeared so that no spectral line can be truly monochromatic. The width of the line is actually produced by a variety of processes. We have included into our considerations natural line broadening, Doppler broadening, Stark broadening and resonance broadening, respectively. These all are subsumed in a normalized line shape $P(\nu, T, p)$. The absorption coefficient of an isolated line i of species a is [21]

$$\kappa^{bb}_{a,i}(\nu, T, p) = \pi r_0 c f^{a,i}_{mn} N^a_n(T, p) P^i(\nu, T, p), \tag{6}$$

where r_0 is the electron radius, c is the velocity of light, $f_{mn}^{a,i}$ is the absorption oscillator strength of the spectral line for electronic transitions between the m and n energy states. $N_n^a(T,p)$ is the population density of the lower electronic energy state and $P^i(\nu,T,p)$ is the normalized line shape. We have used the tabulated values of $f_{mn}^{a,i}$ given by [22]. Only spectral lines having value of the oscillator strength higher than 0.001 have been finally taken into consideration. The line shapes in our calculations are given by convolution of Doppler and Lorentz profiles, resulting in a simplified Voigt profile. For each spectral line we have calculated parameters defining their half-widths and shifts. Semi-empirical formulas given in [15] were used. Absorption coefficient for discrete spectrum of bound-bound transitions takes account of multiplet structures and all overlapping spectral lines of all atoms and ions of the plasma considered.

Spectral coefficients of absorption were calculated in 12 intervals with radiation frequencies spanning from 0.01×10^{15} to 30×10^{15} s^{-1} (10 nm – 30 μm). To distinguish very fine structure of the narrowest lines, each frequency interval was divided into 100,000 integration points. To represent spectral line profiles accurately, the integration points were chosen at the frequencies corresponding to the lines centres. Line wings were accounted for the spectral coefficients of absorption above 10^{-3} of the continuum absorption coefficients.

The statistical weights and energies of the electronic states necessary for calculation of the line absorption coefficients were taken from tables of [20].

Calculated total radiation absorption coefficients as a function of radiation frequency for plasma temperatures of 7000 K and 20 000 K are plotted respectively for the plasma systems of Air+Cu and Air+W in figure 4a) and figure 4b). Strong dependence of the coefficient of the absorption on the radiation frequency makes all integrations over frequency necessary for prediction of radiation heat transfer very time consuming. Dominating continuum radiation in the ultraviolet region of the spectrum can be seen. Both systems of the air plasma with metal admixtures are typical for very large number of spectral lines.

3.3. Molecular absorption - diatomic molecules

In accordance with three types of molecular energy levels - electronic, vibrational and rotational - molecular spectra are very complicated and cover a wide range of electromagnetic waves. The transition frequencies between rotational levels are in the microwave range, the frequencies of transitions between vibrational levels in the infrared region and the frequencies of transitions between electronic levels in visible and ultraviolet spectral region. Therefore, the transitions between electronic states give the main contribution to the radiative heat transfer, and we have considered just the electronic states in our calculations. As a rule, electronic transitions are also accompanied by a change of vibrational and rotational molecular energies. Therefore, the electronic spectra constitute a set of electronic-vibrational bands. Changes in vibrational energy levels often are accompanied by rotational transitions, leading to

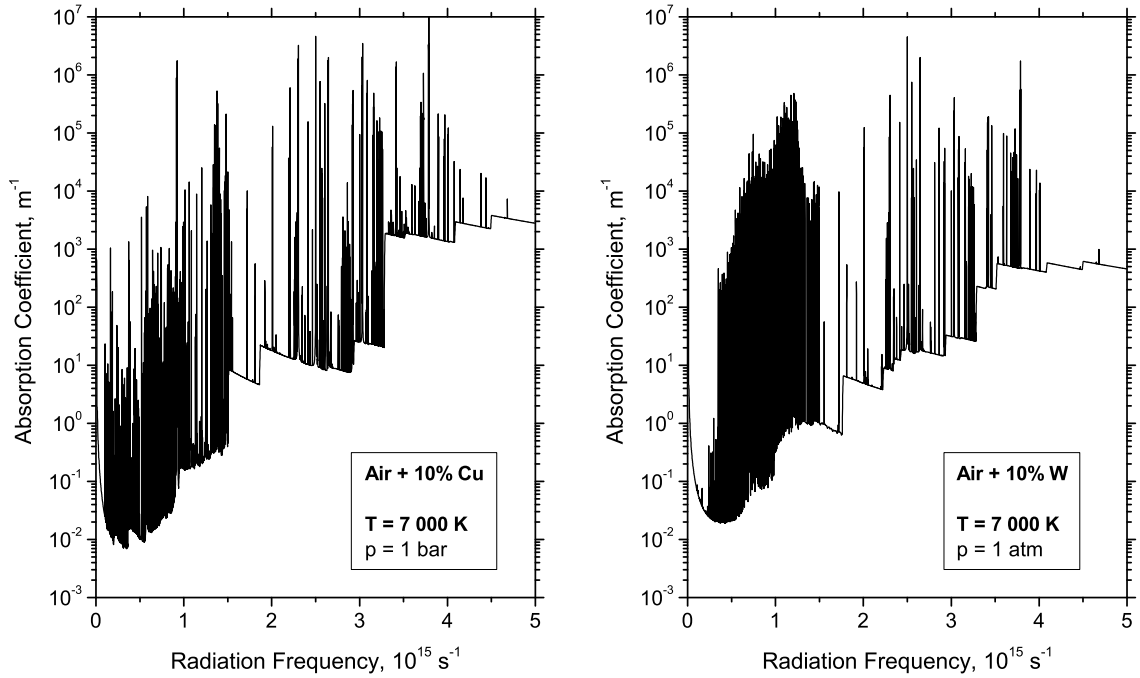

(a) Air+Cu, 7000 K

(b) Air+W, 7000 K

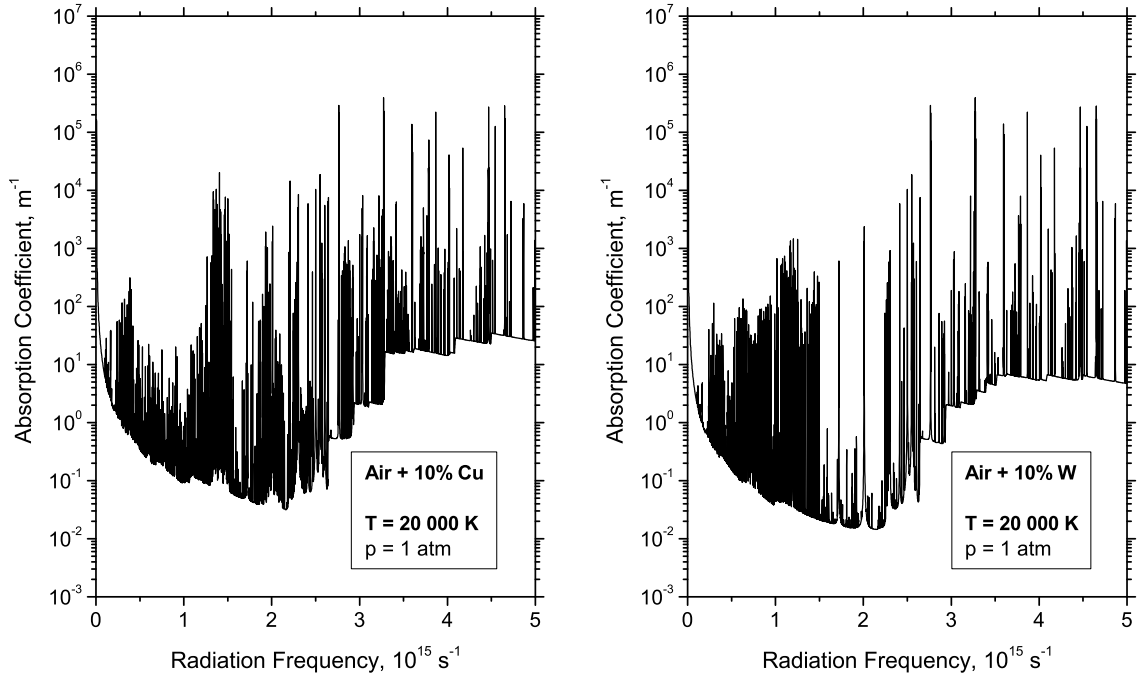

(c) Air+Cu, 20 000 K

(d) Air+W, 20 000 K

Figure 4. Total absorption coefficient for the air plasma with admixtures of Cu and W at temperatures of 7000 K (a,b) and 20 000 K (c,d), respectively.

closely spaced groups of spectral lines that may partly overlap and lead to so-called vibration-rotational bands.

For electronic transitions no selection rules for vibration quantum numbers exist, i.e. transitions between arbitrary vibration levels of the upper and lower electronic states are possible. The theoretical background for the vibrational structure analysis is the Franck-Condon principle [8] that makes it possible to predict the distribution of vibrational band intensities. Relative line intensities in the electronic-vibrational spectra are determined by the Franck-Condon factors

$$\left[\int \psi_{v'}\psi_{v''}\,\mathrm{d}\tau\right]^2 \equiv q_{v'v''} \tag{7}$$

Here, $\psi_{v''}$ and $\psi_{v'}$ are the vibrational wave functions of the lower and higher electronic states, respectively.

The bound-bound absorption coefficient for transition between two vibrational levels v'', v' of two electronic states can be expressed in the form

$$\kappa^{v''v'} = \pi\, r_0 c N_{v''} f_{v''v'} \tag{8}$$

where $N_{v''}$ denotes the number density of the lower vibrational state, and $f_{v''v'}$ the band oscillator strength defined by [24]

$$f_{v''v'} = \frac{\nu_{v''v'}}{3R_\infty c}\frac{\bar{R}_e^2}{g''}q_{v''v'} \tag{9}$$

where R_∞ is the Rydberg constant, g'' the weighting factor of the lower level, $\nu_{v''v'}$ the frequency at which the transition occurs, and $\bar{R}_e^2$ gives the intensity distribution in electronic structure. For approximate calculation of radiative properties, it is useful to define the spectral absorption coefficient for the band system averaged through the rotational spectrum, and also partially smeared through the vibrational structure

$$\bar{\kappa}_\nu = N\sigma\left(\nu, T\right) = N\pi\, r_0 \frac{\nu}{3R_\infty c}\frac{\bar{R}_e^2}{g''}\frac{1}{\Delta\omega}\sum_{v''v'} q_{v''v'}w_{v''} \tag{10}$$

Here, N is the molecular number density, ν the radiation frequency of absorbed photon, and $w_{v''}$ denotes the Boltzman probability of the occupation of the lower vibrational level. The sum of Franck-Condon factors is performed for all transitions $v'' \to v'$ with

$$\omega_{v'} - \omega_{v''} \equiv \omega_{v''v'} \in \left\langle \omega - \frac{\Delta\omega}{2},\, \omega + \frac{\Delta\omega}{2} \right\rangle \tag{11}$$

where $\Delta\omega$ is interval of averaging around $\omega = \nu/c$. The Franck-Condon factors are tabulated for many molecular transitions in [25], or they can be calculated by computer code [26].

4. Air + Cu

The system Air+Cu comprised the elements of C, N, O, Ar, Cu, e^- and their various compounds. It was found that the system is heterogeneous for low temperatures at all supposed variants. The system can be treated as gaseous for all temperatures $T > T_{\text{tran}}$ where T_{tran} depends on the pressure and the amount of the copper in the system. The temperature of the phase transition as a function of the plasma pressure is given in the following table:

Table 4. Temperature of the phase transition in 3 variants of Air+Cu plasma system for various plasma pressures.

p (bar)	variant		
	1	2	3
1	2059.3	2228.7	2312.5
2	2141.7	2326.5	2418.4
5	2263.2	2472.3	2577.0
10	2364.0	2594.8	2711.1
20	2473.4	2729.3	2859.3

For the sake of simplicity, we have included into our calculation of the net emission coefficients the following species: N, N^+, N^{2+}, N^{3+}, O, O^+, O^{2+}, O^{3+}, C, C^+, C^{2+}, C^{3+}, Ar, Ar^+, Ar^{2+}, Ar^{3+}, N_2, N_2^+, O_2, O_2^+, O_3, C_2, C_2^+, C_2^-, NO, NO^+, N_2O, NO_2, CN, CN^+, CO_2, CO, CO^+ and Cu, Cu^+, CuO, Cu_2. Ions of Cu^{++} and higher have not been accounted for as there is no available spectral data in the literature.

Photo-ionization cross sections for the ground states of neutral atoms and ions of N, O, Ar, and C were calculated using analytic fits of theoretical cross sections from the "Opacity Project" [17]. The cross sections for following excited levels of neutral atoms were calculated using the quantum defect method of Burges and Seaton [18]: Oxygen - 3s, 3p, 4s, and 4p states, Nitrogen - 3s and 3p states, Carbon - 3s, 3p, 4s, and 4p states. All other excited states of N, O, Ar, C, Cu and the ground state of Cu were treated using Coulomb approximation for hydrogen-like species [19]. We have taken into consideration 484 energy levels and 11 861 spectral lines of pure air, 115 energy levels and 3 370 spectral lines of carbon, and 217 energy levels and 1 910 spectral lines of copper.

Molecular photo-absorption coefficients of diatomic molecules were calculated using approximation according to Equation (10). Required input data for the calculation were taken from [23]. This concerns to the following diatomic molecules and electronic transitions: $O_2(X^3\Sigma_g^- \rightarrow B^3\Sigma_u^-)$, O_2^+ $(X^2\Pi_g \rightarrow A^2\Pi_u)$, N_2 $(B^3\Pi_g \rightarrow A^3\Sigma_u, C^3\Pi_u \rightarrow B^3\Pi_g)$, N_2^+ $(B^2\Sigma_u^+ \rightarrow X^2\Sigma_g^+, A^2\Pi_u \rightarrow X^2\Sigma_g^+)$, NO $(B^2\Pi_r \rightarrow X^2\Pi_r, A^2\Sigma^+ \rightarrow X^2\Pi_r)$, NO^+ $(A^1\Pi \rightarrow X^1\Sigma^+)$, C_2 $(a^3\Pi \rightarrow d^3\Pi)$, C_2^+ $(X^2\Pi \rightarrow A^2\Sigma_g^-)$, $C_2^-(X^2\Sigma_g^+ \rightarrow B^2\Sigma_u^+)$, CO $(b^3\Sigma \rightarrow a^3\Pi, B^1\Sigma \rightarrow A^1\Pi)$, CO^+ $(X^2\Sigma^+ \rightarrow A^2\Pi, X^2\Sigma^+ \rightarrow B^2\Sigma^+)$, CN $(X^2\Pi \rightarrow A^2\Pi, X^2\Sigma \rightarrow B^2\Sigma)$, CN^+ $(X^1\Sigma^+ \rightarrow F^1\Sigma^+)$, Cu_2 $(X^1\Sigma_g^+ \rightarrow B^1\Sigma_u^+)$, CuO $(X^2\Pi \rightarrow A^2\Sigma, X^2\Pi \rightarrow$

$E^2\Delta$, $X^2\Pi \rightarrow G^2\Sigma$). Photo-absorption cross sections of polyatomic molecules O_3, N_2O and NO_2 were taken from [27, 28] and for CO_2 from [29, 30, 31].

5. Air + W

The composition of the system Air+W was similar to the Air+Cu with Cu replaced by species of W. It was found that the system is heterogeneous for low temperatures at all supposed variants. The system can be treated as gaseous for all temperatures $T > T_{\text{tran}}$ where T_{tran} depends on the pressure and the amount of the tungsten in the system. The temperature of the phase transition is given in the following table:

Table 5. Temperature of the phase transition in 3 variants of Air+W plasma system for various plasma pressures.

p (bar)	variant		
	1	2	3
1	1666.6	1759.3	1854.2
2	1700.6	1841.2	1949.5
5	1750.6	1970.3	2102.7
10	1833.0	2086.8	2244.9
20	1927.1	2225.7	2419.9

For the sake of simplicity, we have included into our calculation of the net emission coefficients the following species: N, N^+, N^{2+}, N^{3+}, O, O^+, O^{2+}, O^{3+}, C, C^+, C^{2+}, C^{3+}, Ar, Ar^+, Ar^{2+}, Ar^{3+}, N_2, N_2^+, O_2, O_2^+, O_3, C_2, C_2^+, C_2^-, NO, NO^+, N_2O, NO_2, CN, CN^+, CO_2, CO, CO^+ and W, W^+, WO. Unfortunately, there is no additional spectral data for higher ions and molecular species of tungsten.

Photo-ionization cross sections of W and W^+ were treated using Coulomb approximation for hydrogen-like species. In addition to energy levels and spectral lines of pure air and carbon, 47 energy levels and 1 181 spectral lines of wolfram were taken into account. In molecular photo-absorption, instead of CuO molecule the photo-absorption of molecule WO in electronic transition $X^1 0^+ \rightarrow D1$ was treated [23].

6. Net Emission Coefficients

On making the assumption of the local thermodynamic equilibrium coefficient of absorption κ_ν is related to the coefficient of emission ε_ν by Kirchhoff's law

$$\varepsilon_\nu = B_\nu \kappa_\nu, \tag{12}$$

where B_ν is the Planck function. Strong self-absorption of the radiation in the plasma volume occurs and this must be taken into account in calculations. The net emission coefficient of radiation, ε_{N_ν} is defined by Lowke [8] as

$$\varepsilon_{N_\nu} = \varepsilon_\nu - J_\nu \kappa_\nu, \tag{13}$$

where J_ν is an average radiation intensity which is a function of the plasma temperature. For an isothermal sphere it is defined as

$$J_\nu = B_\nu \left[1 - \exp\left(-\kappa_\nu R\right)\right]. \tag{14}$$

Combination of Equation (13) and (14) gives the expression for the net emission coefficient of radiation

$$\varepsilon_N = \int_0^\infty B_\nu \kappa_\nu \exp(-\kappa_\nu R) \mathrm{d}\nu. \tag{15}$$

The "isothermal" net emission coefficient, ε_N, corresponds to the fraction of the total power per unit volume and unit solid angle irradiated into a volume surrounding the axis of the arc plasma and escaping from the arc column after crossing a thickness R of the isothermal plasma. Application of the net emission coefficients to a prediction of energy balance gives good results for central arc temperatures, however it cannot predict accurate temperature profiles at low temperatures near the edge of the arc, because of the absorption of ultraviolet radiation emitted at the centre of the arc at high temperatures.

Examples of calculated temperature dependence of the net emission coefficients for various radii of a plasma cylinder of Air + 10 vol% Cu and Air + 10 vol% W are presented respectively in figure 5a) and figure 5b). Radius $R = 0$ corresponds to omitting of self-absorption of radiation. Beside the temperature dependence, the strong effect of the plasma thickness can be seen from the figures. Moreover, very large number of spectral lines in plasmas with metals also contribute to the higher emissivity of the plasma.

Effect of the proportion of metal vapour to the air plasma on the net emission coefficients is shown in figure 6a) and figure 6b). Net emission coefficients of plasmas of Air+Cu and Air+W for the radius of 0.1 cm at a pressure of 1 atm are compared. Admixture of copper or tungsten increases net emission coefficients, especially at low temperatures. This can be explained by lower ionization energy of the metal atoms and ions in comparison with other considered species. In case of a tungsten admixture at temperatures above 15 000 K, the contribution of the metal species to the value of the net emission coefficient is almost negligible. It is due to lower cross sections of photo-recombination of W^+ ions in comparison with Cu^+ ions.

Comparisons of net emission coefficients calculated in three composition variants of 1, 5 and 10 volume percent of Cu or W respectively for radius R = 0.1 cm at a pressure of 1 atm are presented in figure 6. Presence of metal vapour in the air plasma tends to increase the net emission coefficients mainly for temperatures between 5000 to 10 000 K. This is due to lower ionization energy of Cu and W in comparison with N and O leading to higher concentration of electrons. Due to lack of data for higher ions of copper and tungsten, net emission coefficients above 20 000 K are rather underestimated.

Figure 8 shows a comparison of our values Air+1% Cu net emission coefficients with those of [1] at a pressure of 1 atm for radii of R = 0.1 cm (a) and R = 0 (b). The latter corresponds to fictitious case of an optically thin plasma without self-absorption.

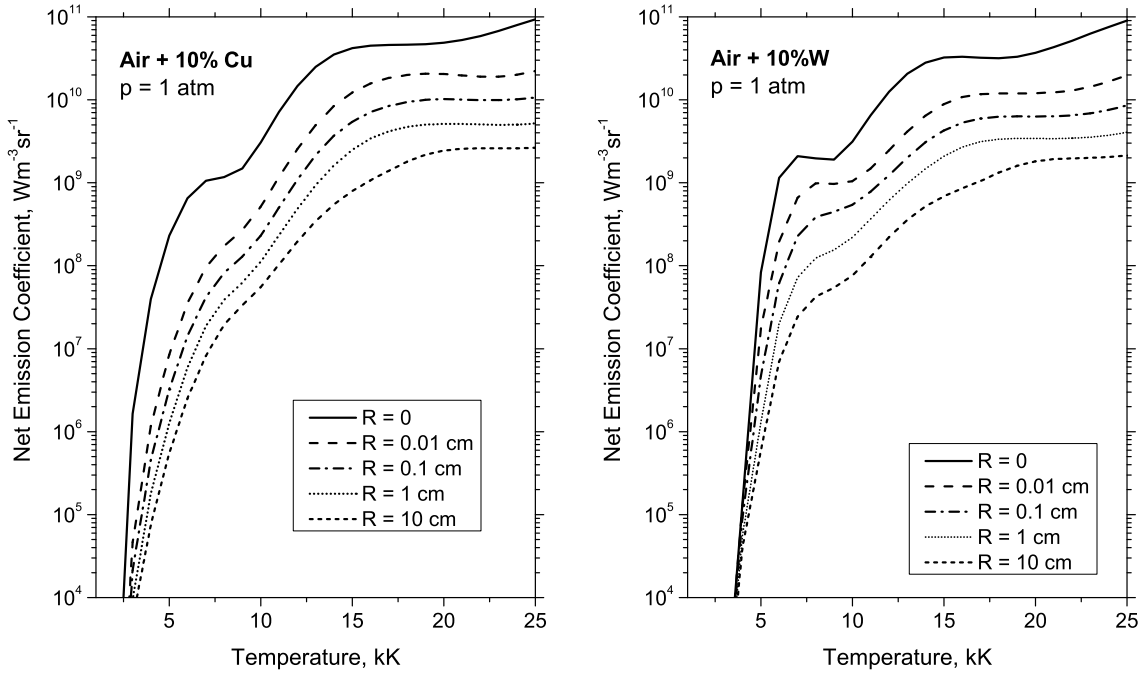

(a) Air+Cu (b) Air+W

Figure 5. Net emission coefficient of air plasma with 10 vol% of Cu and W at 1 atm for various R.

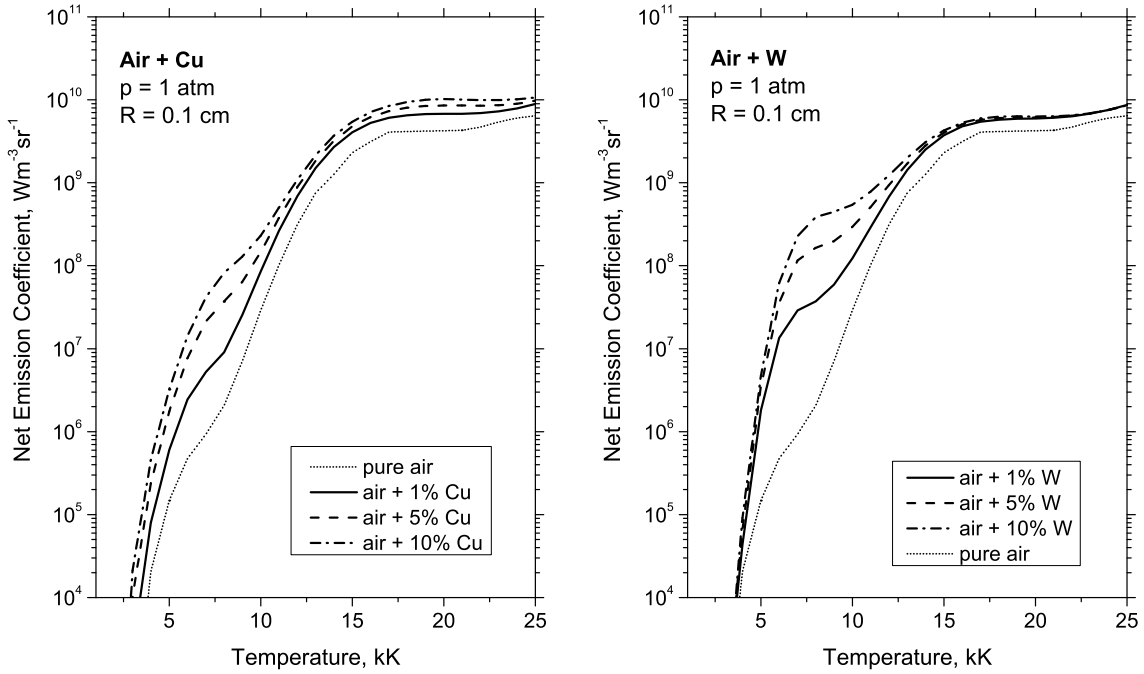

(a) Air+Cu (b) Air+W

Figure 6. Net emission coefficient of air plasma with various mixtures of Cu and W (R=0.1 cm, p=1 atm).

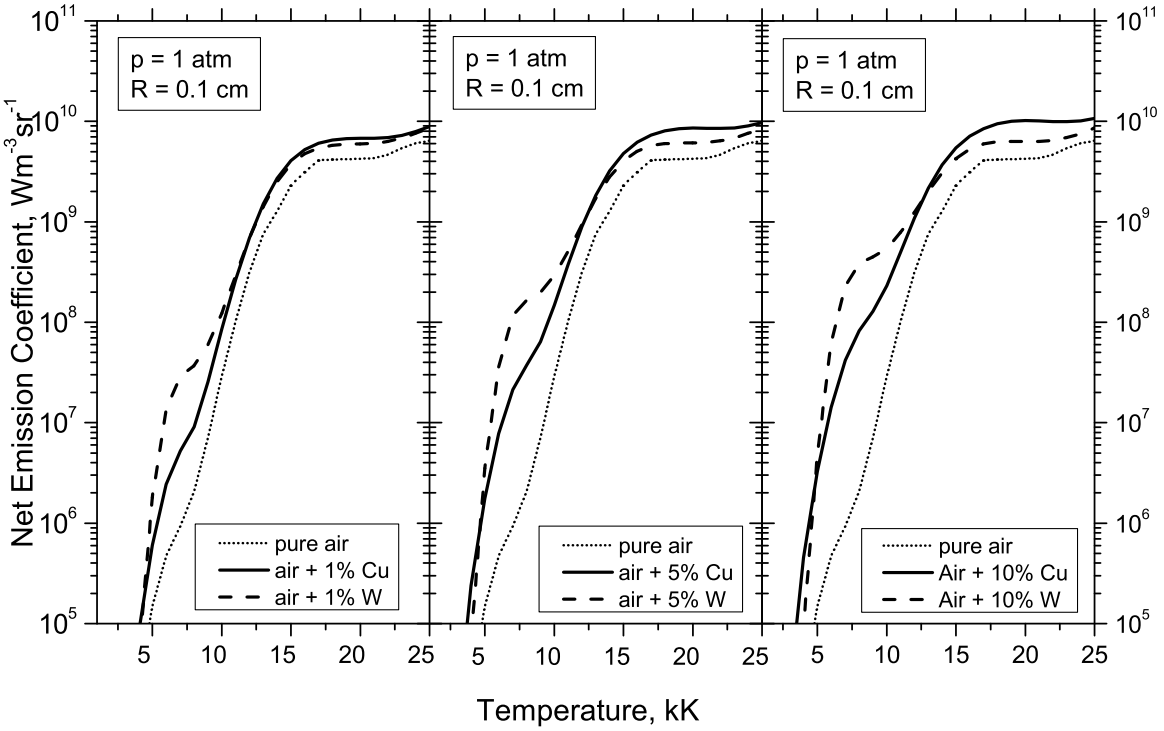

Figure 7. Net emission coefficients for three composition variants of 1, 5 and 10 vol% of Cu or W (R=0.1 cm, p=1 atm.)

Differences in the results can be explained by different input spectral data (oscilator strengths and cross sections of photo-ionization) and by different treatment of spectral line overlapping which is omitted in [1]. It was reported in our previous paper [16] that neglecting the spectral lines overlapping gives higher net emission coefficients by up to 70%.

The total radiation from all wavelengths is crucial to get the central arc temperature right. But the fraction that gets out of the arc, i.e. the fraction which is largely in the visible, is crucial for total energy balance calculations to calculate the energy which goes out of the arc. It can be seen from figure 3 and 4 that the ultraviolet absorption coefficient at low plasma temperature is much more higher in comparison with the one in the visible region. Thus ultraviolet radiation is absorbed by the cold gas at the arc edge within short distance of about 10^{-1} cm, where a very steep temperature gradient occurs. In figure 10a) and figure 10b) we show fraction of the net emission coefficients of wavelength less then 2.5×10^{15} s^{-1} (120 nm) for various admixtures of Cu and W. In both figures the more amount of a metal admixture the less fraction of radiation. The fraction increases with the plasma temperature, whereas below 5000 K it is less then 0.05. Effect of the plasma thickness on the fraction of radiation is presented in figure 10. Only absorption in the outer region of the arc of any significance is the photoionization of the ground state. So the fraction of radiation that is absorbed at the edge of the

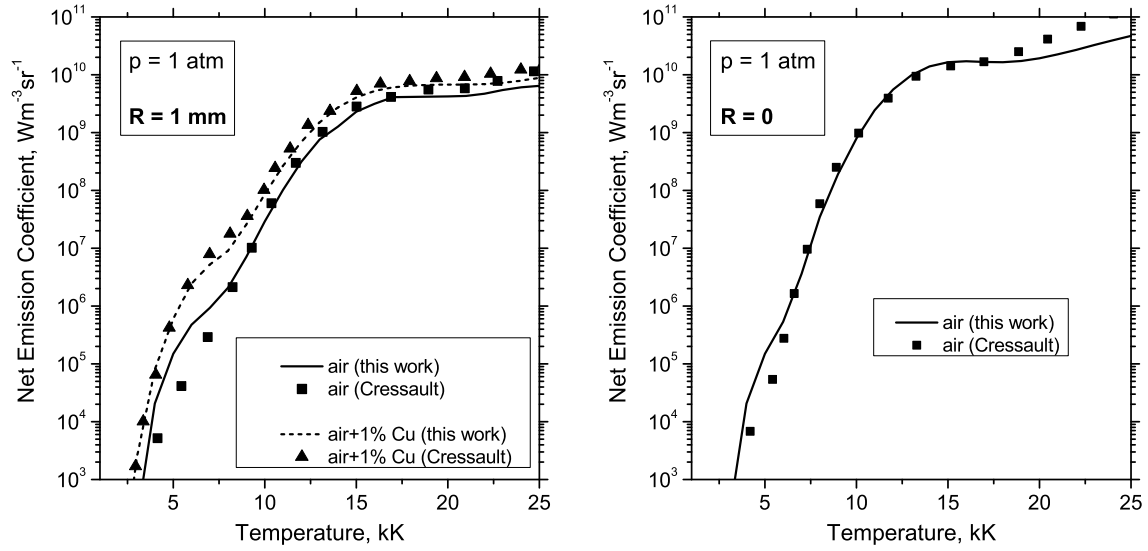

(a) R = 0.1 mm (b) R = 0

Figure 8. Comparison of calculated net emission coefficients with Ref. [1].

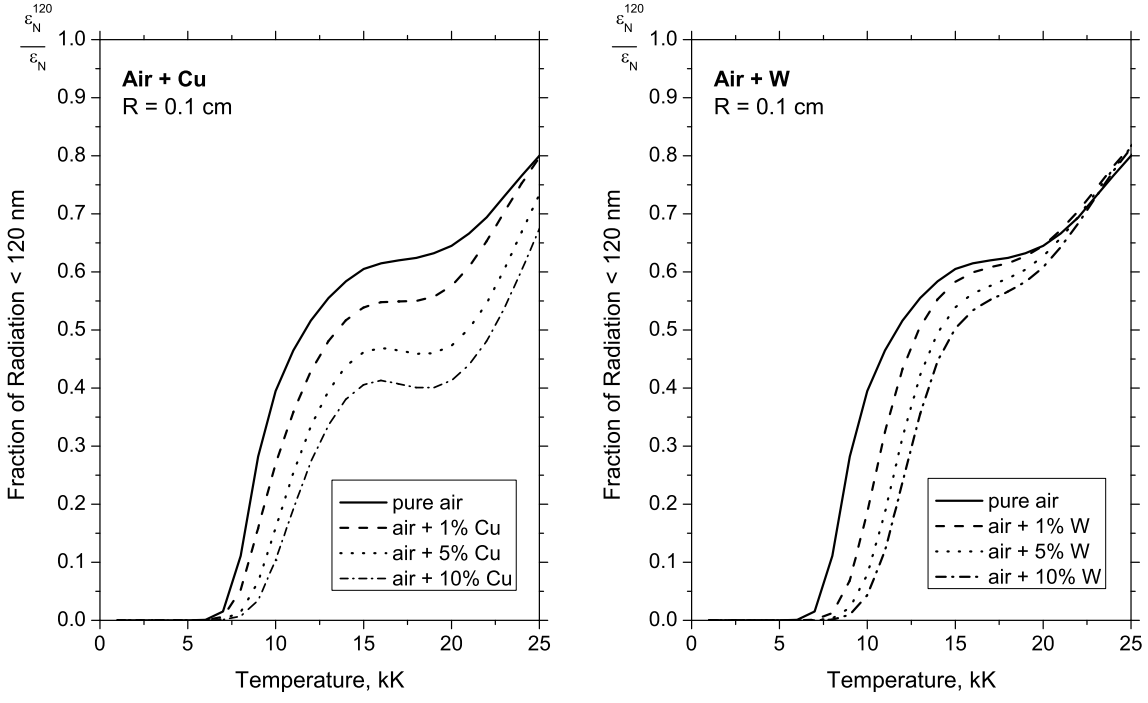

(a) Air+Cu (b) Air+W

Figure 9. Fraction of radiation for air plasma with various admixtures of Cu and W.

arc is only that by the ground state and is simply the fraction of the radiation that has wavelengths less than the photoionization threshold.

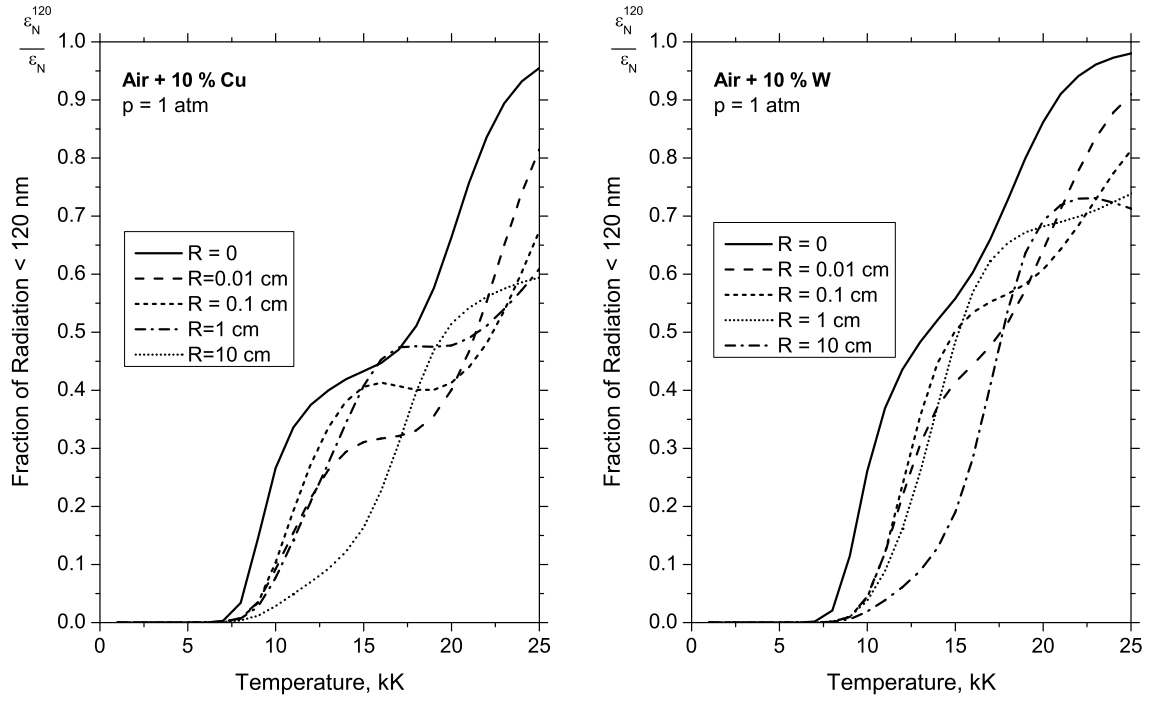

(a) Air+Cu (b) Air+W

Figure 10. Fraction of radiation for air plasma with 10% of Cu and W at various plasma thicknesses.

Effect of the plasma pressure on the net emission coefficients of Air+Cu and Air+W plasma systems is compared in figure 11 for the plasma pressures up to 20 bars. In both cases, increasing the pressure leads to the higher net emission coefficients at all temperatures. Net emission coefficients are proportional to population densities of energy levels in atoms and ions which increase with the pressure.

7. Conclusions

Calculations of the net emission coefficients for thermal plasmas of air with various admixtures of copper and tungsten vapour have been performed as a function of temperature. Both continuum and line radiation in the interval from infrared to the ultraviolet portion of the spectrum were taken into account. The net emission coefficients were calculated for temperatures up to 25 000 K assuming local thermodynamic equilibrium. It is shown that the metallic vapours modify the values of net emission coefficients. Increasing effect of a metal admixture to the net emission coefficients of the air plasma is presented. In addition, results are presented of the fraction of the radiation that is less than threshold of 120 nm.

The calculations of the net emission coefficients assume an isothermal plasma. Consequently, approximation of the radiation losses by using the net emission coefficients is valid only near the arc axis. It has been reported in [8] that using the net emission

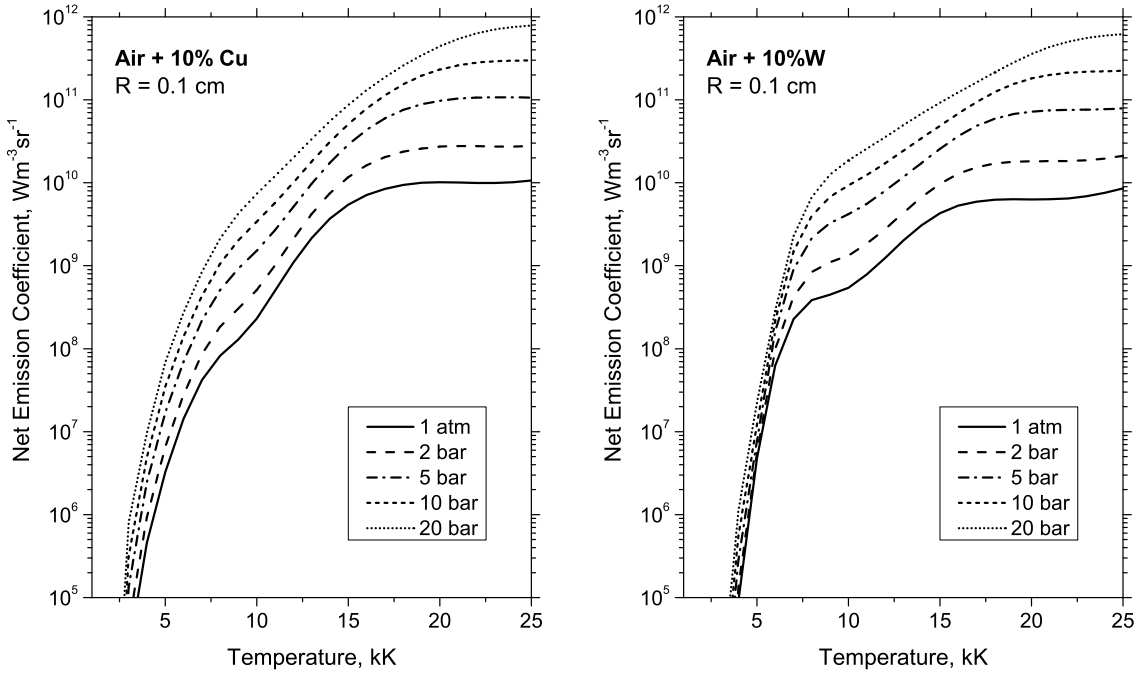

(a) Air+Cu (b) Air+W

Figure 11. Net emission coeffcients as a function of pressure for air with admixtures of Cu and W.

coefficients in prediction of arc temperature profiles yields central arc temperatures accurate to 10 per cent. The advantage of using net emission coefficients for prediction of radiation transport is rather computational simplicity, thus low computation cost.

In the outer and cooler parts of the arc plasma, predictions of radiation using the present net emission coefficients will not be accurate and other approximation must be used, for example the method of partial characteristics [7, 32, 33].

Acknowledgments

This work has been supported by the Ministry of Education, Youth and Sports under projects No. MSM0021630516 and CZ.1.05/2.1.00/01.0014.

References

[1] Cressault Y, Hannachi R, Teulet Ph, Gleizes A, Gonnet J-P and Battandier J-Y 2008 *Plasma Sources Sci. Technol.* **17** 1–9
[2] Gleizes A, Gonzales J J, Liani B and Raynal G 1993 *J.Phys. D: Appl. Phys.* **26** 1921–1927
[3] Menart J and Malik S 2002 *J.Phys. D: Appl. Phys.* **35** 867–874
[4] Cram L E 1985 *J.Phys. D: Appl. Phys.* **18** 401–411
[5] Essoltani A, Proulx P, Boulos M I and Gleizes A 1994 *Plasma Chem. Plasma Processing* **14** 437–450
[6] Shayler P J and Fang M T C 1977 *J.Phys. D: Appl. Phys.* **10** 1659

[7] Aubrecht V and Lowke J J 1994 *J.Phys. D: Appl. Phys.* **27** 2066–2073
[8] Lowke J J 1974 *JQSRT* **14** 111–122
[9] Naghizadeh-Kashani Y, Cressault Y and Gleizes A 2002 *J.Phys. D: Appl. Phys.* **35** 2925–2934
[10] Aubrecht V and Bartlova M 2009 *Plasma Chem. Plasma Processing* **29** 131–147
[11] Lindmayer M, Mutzke A, Rüther T and Springstubbe M 2005 *Proc. XVIth Symposium on Physics of Switching Arc* (Ski Hotel - Nove Mesto) vol II (Brno - Letohrad) 278–292
[12] Zhang J F, Fang M T C and Newland D B 1987 *J. Phys. D: Appl. Phys.* **20** 368–379
[13] Coufal O, Sezemsky P and Zivny O 2005 *J.Phys. D: Appl. Phys.* **38** 1265–1274
[14] Lide D R (Editor-in-Chief) *Handbook of Chemistry and Physics.* 88th Edition (CRC Press: Bocca Raton) 2007–2008
[15] Liebermann R W and Lowke J J 1976 *JQSRT* **16** 253–264
[16] Aubrecht V and Gross B 1994 *J Phys D: Appl. Phys.* **27** 95–100
[17] Verner D A, Ferland G J and Korista K T 1996 *Astrophysical Journal* **465** 487/-492
[18] Burgess A and Seaton M 1958 *Rev.Mod.Phys.* **30** 992/-1003
[19] Sobel'man I I 1979 *Atomic Spectra and Radiation Transitions* (Berlin :Springer Verlag)
[20] Ralchenko Y, Kramida A E, Reader J and NIST ASD team 2008 *NIST Atomic spectra database (version 3.1.5)* available online at [http://physics.nist.gov/] National Institute of Standards and Technology Gaithersburg MD 2009
[21] Griem H R 1967 *Plasma Spectroscopy* (New York: McGraw-Hill)
[22] Kurucz R L and Peytremann E Atomic line data (R.L. Kurucz and B. Bell) Kurucz CD-ROM N0.23 Cambridge, Mass.: Smithsonian Astrophysical Observatory, available online at [http://cfa-www.harvard.edu/amp/ampdata/kurucz23/sekur.html] 1995
[23] Herzberg G 1979 *Molecular Spectra and Molecular Structure. IV. Spectra of Diatomic Molecules* (New York: D. Van Nostrand Co)
[24] Mnacakanjan A Ch 1968 *TVT* **6** 236–241
[25] Kuzmenko N E, Kuznecova L A Kuzjakov J J 194 *Faktory Franka-Kondona dvuchatomnych molekul* (Moskva: Izd. Moskovskogo universiteta)
[26] Stakhursky V L [http://www.chemistry.ohio-state.edu/ṽstakhur]
[27] Atkinson et al, 1997 *J. Phys. Chem. Ref. Data* **26** 1329–1498
[28] Dishoeck van E F 1998 in *Rate Coefficients in Astrochemistry* eds. Millar T J and Williams D A (Kluwer) 49–72
[29] HITRAN database [http://cfa-www,harvard,edu/HITRAN/]
[30] Chan W F Cooper G and Brion C E 1993 *Chem. Phys.* **178** 401–413
[31] Berkowitz J 2002 *Atomic and Molecular Photoabsorption* (New York: Academic Press)
[32] Raynal G and Gleizes A 1995 *Plasma Sources Sci. Technol.* **4** 152–160
[33] Dixon C M and Fang M T C 2003 *J. Phys. D: Appl. Phys.* **36** 2767–2773